Pd-(MOP) Chemistry: Novel Bonding Modes and Interesting Charge Distribution

Pascal Dotta, P. G. Anil Kumar, and Paul S. Pregosin*

Laboratory of Inorganic Chemistry, ETHZ, Hönggerberg, CH-8093 Zürich

Alberto Albinati* and Silvia Rizzato

Department of Structural Chemistry (DCSSI), University of Milan, 20133 Milan, Italy

Received July 28, 2003

The new Pd-MOP acetyl acetonate complexes [Pd(acac)(**10a** or **10b**)]BF_4, **12a**,**b**, were prepared starting from [Pd(acac)$(CH_3CN)_2$]BF_4, whereas [Pd(acac)(**11**-H)], **13**, was obtained directly from $Pd(acac)_2$ by adding **11**. [Ligand **10a**, MeO-MOP = (*R*)-2-(diphenylphosphino)-2′-methoxy-1,1′-binaphthyl; ligand **11**, HO-MOP = (*R*)-2-(diphenylphosphino)-2′-hydroxy-1,1′-binaphthyl]. The solid-state structures for cationic **12a** and neutral **13** were determined via X-ray diffraction methods and reveal that both structures contain Pd−C σ-bonds arising from the MOP naphthyl backbone. In structure **13**, the hydroxyl function in **11** has lost a proton to afford a keto-anionic chelating ligand. ^{13}C NMR studies confirm that the solution structures are the same as those found in the solid state and, for **12**, describe how the organic cation distributes the positive charge.

Introduction

The chiral biaryl-based bidentate phosphine auxiliaries Binap, **1**, and MeO-Biphep, **2** (see Scheme 1), are now in common use in enantioselective homogeneous catalysis.[1] Hayashi and co-workers,[2] in a series of fine papers, have pointed out that the MOP auxiliaries, e.g., **3** and **4**, provide a useful monodentate alternative to Binap.

One member of the MOP class, MAP, **5**, introduced by Kocovsky[3] and Ding,[4] has been shown to display an unexpected bonding mode. Primarily, the MAP ligand tends to form complexes of Pd(II) in which there is a σ-bond from the ipso carbon, C1, to the metal. A structural fragment demonstrating this type of interaction is shown in Scheme 2, as **6**, where the positive charge resides primarily on the nitrogen atom.[3,4] The MeO-MOP compound, **10**, is thought to prefer a bonding mode in which the C1−C6 double bond is π-complexed, i.e., a phosphine-olefin chelate ligand as in **7**.[3b] In some ways, **7** is not surprising, as Binap and MeO-Biphep both complex this double bond rather readily in Ru(II) chemistry, e.g., **8**.[5−7]

The interest in how the MOP donor binds a transition metal is related to the question of chirality transfer. It would be useful to know if the MOP class favors chelation, rather than a monodentate mode. In the latter situation, a relatively rigid chiral pocket might arise via restricted rotation around M−P and/or P−C bonds. Alternatively, perhaps two MOP ligands may complex in order to form a sterically crowded pocket.

We show here that, with Pd(II), the MeO-MOP ligands **10** can indeed demonstrate structures similar

(1) Kitamura, M.; Tsukamoto, M.; Bessho, Y.; Yoshimura, M.; Kobs, U.; W. M.; Noyori, R. *J. Am. Chem. Soc.* **2002**, *124*, 6649−6667. Brunkan, N. M.; Gagne, M. R. *Organometallics* **2002**, *21*, 1576−1582. Abdur-Rashid, K.; Faatz, M.; Lough, A. J.; Morris, R. H. *J. Am. Chem. Soc.* **2001**, *123*, 7473−7474. Wiles, J.; Bergens, S. H. *J. Am. Chem. Soc.* **1997**, *119*, 2940−2941. Crameri, Y.; Foricher, J.; Hengartner, U.; Jenny, C.; Kienzle, F.; Ramuz, H.; Scalone, M.; Schlageter, M.; Schmid, R.; Wang, S. *Chimia* **1997**, *51*, 303. Kumobayashi, H. *Rec. Trav. Chim. Pays-Bas* **1996**, *115*, 201−210. Sperrle, M.; Gramlich, V.; Consiglio, G. *Organometallics* **1996**, *15*, 5196−5201. Zhang, X.; Mashima, K.; Koyano, K.; Sayo, N.; Kumobayashi, H.; Akutagawa, S.; Takaya, H. *J. Chem. Soc., Perkin Trans.* **1994**, 2309−2322. Mezzetti, A.; Tsachumper, A.; Consiglio, G. *J. Chem. Soc., Dalton Trans.* **1995**, 49.

(2) Shimada, T.; Mukaide, K.; Shinohara, A.; Han, J. W.; Hayashi, T. *J Am. Chem. Soc.* **2002**, *124*, 1584−1585. Hayashi, T.; Han, J. S.; Takeda, A.; Tang, J.; Nohmi, K.; Mukaide, K.; Tsuji, H.; Uozumi, Y. *Adv. Synth. Catal.* **2001**, *343*, 279−283. Hayashi, T.; Hirate, S.; Kitayama, K.; Tsuji, H.; Torii, A.; Uozumi, Y. *J. Org. Chem.* **2001**, *66*, 1441−1449. Hayashi, T. *Acc. Chem. Res.* **2000**, *33*, 354−362. Hayashi, T.; Hirate, S.; Kitayama, K.; Tsuji, H.; Torii, A.; Uozumi, Y. *Chem. Lett.* **2000**, 1272−1273. Hayashi, T.; Kawatsura, M.; Uozumi, Y. *J. Am. Chem. Soc.* **1998**, *120*, 1681−1687. Uozumi, Y.; Danjo, H.; Hayashi, T. *Tetrahedron Lett.* **1998**, *39*, 8303−8306. Uozumi, Y. *Yakugaku Zasshi-J. Pharm. Soc. Jpn.* **1998**, *118*, 193−205. Hayashi, T. *Acta Chem. Scand.* **1996**, *50*, 259−266. Hayashi, T. *J. Synth. Org. Chem. Jpn.* **1994**, *52*, 900−911. Uozumi, Y.; Kitayama, K.; Hayashi, T. *Tetrahedron Asym.* **1993**, *4*, 2419−2422.

(3) (a) Kocovsky, P.; Vyskocil, S.; Smrcina, M. *Chem. Rev.* **2003**, *103*, 3213−3245. (b) Lloyd-Jones, G. C.; Stephen, S. C.; Murray, M.; Butts, C. P.; Vyskocil, S.; Kocovsky, P. *Chem. Eur. J.* **2000**, *6*, 4348−4357. (c) Fairlamb, I. J. S.; Lloyd-Jones, G. C.; Vyskocil, S.; Kocovsky, P. *Chem. Eur. J.* **2002**, *8*, 4443−4453. (d) Kocovsky, P.; Malkov, A. V.; Vyskocil, S.; Lloyd-Jones, G. C. *Pure Appl. Chem.* **1999**, *71*, 1425−1433. (e) Kocovsky, P.; Vyskocil, S.; Cisarova, I.; Sejbal, J.; Tislerova, I.; Smrcina, M.; Lloyd-Jones, G. C.; Stephen, S. C.; Butts, C. P.; Murray, M.; Langer, V. *J. Am. Chem. Soc.* **1999**, *121*, 7714−7715. (f) Vyskocil, S.; Smrcina, M.; Hanus, V.; Polasek, M.; Kocovsky, P. *J. Org. Chem.* **1998**, *63*, 7738−7748. (g) Vyskocil, S.; Smrcina, M.; Kocovsky, P. *Tetrahedron Lett.* **1998**, *39*, 9289−9292.

(4) (a) Wang, X. P.; Li, X.; Sun, J.; Ding, K. *Organometallics* **2003**, *22*, 1856−1862. (b) Ding, K.; Wang, Y.; Liu, J.; Yun, H.; Wu, Y.; Ferada, M.; Okubo, Y.; Mikami, K. *Chem. Eur. J.* **1999**, *5*, 1734−1737.

(5) Aneetha, H.; Jemenez-Tenorio, M.; Puerta, M. C.; Valerga, P.; Mereiter, K. *Organometallics* **2002**, *21*, 628−635.

(6) Geldbach, T. J.; Drago, D.; Pregosin, P. S. *J. Organomet. Chem.* **2002**, *643*, 214−222. Geldbach, T. J.; Pregosin, P. S. *Eur. J. Inorg. Chem.* **2002**, 1907−1918. Geldbach, T. J.; Pregosin, P. S.; Albinati, A. *Organometallics* **2003**, *22*, 1443−1451. Geldbach, T. J.; Pregosin, P. S.; Albinati, A.; Rominger, F. *Organometallics* **2001**, *20*, 1932−1938.

(7) Feiken, N.; Pregosin, P. S.; Trabesinger, G.; Albinati, A.; Evoli, G. L. *Organometallics* **1997**, *16*, 5756−5762. Feiken, N.; Pregosin, P. S.; Trabesinger, G.; Scalone, M. *Organometallics* **1997**, *16*, 537.

10.1021/om030555d CCC: $25.00
Publication on Web 11/07/2003

Scheme 1. Chiral Biaryl-Based Phosphine Ligands

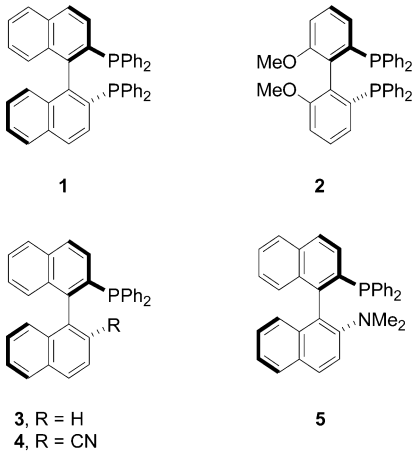

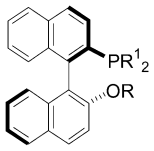

10a, R = Me, R^1 = Ph
10b, R = Me, R^1 = 3,5-di-t-butylphenyl
11, R = H, R^1 = Ph

Scheme 2. Structural Fragments Showing the Various Bonding Modes

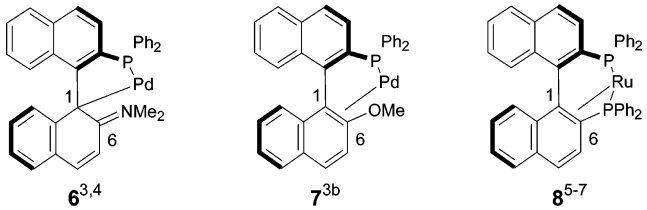

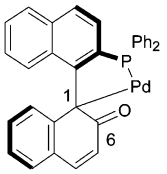

9

to **6** and that the HO-MOP ligand, **11**, carries this tendency much further and affords the keto-anion structure, **9**.

Results and Discussion

Solid-State Structures. The new acetyl acetonate complexes [Pd(acac)(**10a** or **10b**)]BF_4, **12a**,**b**, and [Pd(acac)(**11-H**)], **13**, were prepared as shown in Scheme 3. In the preparation of **13** one acac ligand functions as a base. The solid-state structures for cationic **12a** and neutral **13** were determined via X-ray diffraction methods, and views of these are shown in Figures 1 and 2, with a summary of the most salient bond distances and bond angles in Table 1.

The immediate coordination sphere of both complexes consists of the two acac Pd−O interactions and the P,C

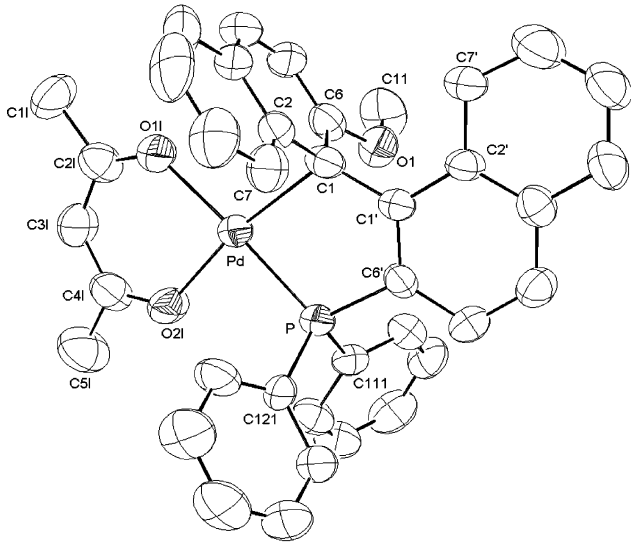

Figure 1. ORTEP view of the cation of **12a**.

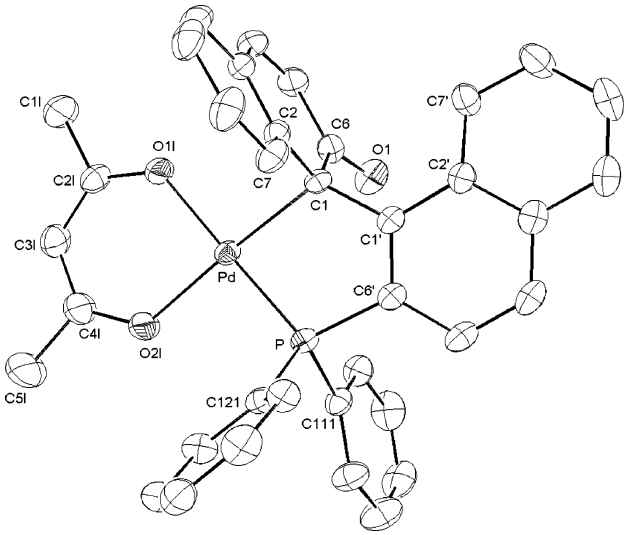

Figure 2. ORTEP view of **13**.

Scheme 3

$$Pd(acac)_2 + HBF_4 \xrightarrow[\text{- Hacac}]{CH_3CN} [Pd(acac)(CH_3CN)_2]BF_4 \quad (1)$$

$$[Pd(acac)(CH_3CN)_2]BF_4 \xrightarrow[\text{- 2 } CH_3CN]{\textbf{10}} [Pd(acac)(\textbf{10})]BF_4\ \ \textbf{12} \quad (2)$$

$$Pd(acac)_2 \xrightarrow[\text{- Hacac}]{\textbf{11}} [Pd(acac)(\textbf{11-H})]BF_4\ \ \textbf{13} \quad (3)$$

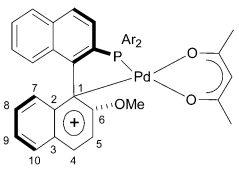

12a Ar = Phenyl
12b Ar = 3,5-di-^{t}Bu-phenyl

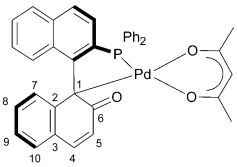

13

chelate with both structures revealing Pd−C σ-bonds. The local geometries can be considered as distorted square planar, with bond angles varying from the classical values by as much as ca. 10°.

Table 1. Bond Lengths (Å) and Angles (deg) for Pd(II) Compounds 12a and 13

	12a	13
	Bond Lengths	
Pd1−P1	2.219(2)	2.1938(6)
Pd1−O1L	2.040(6)	2.057(2)
Pd1−O2L	2.052(6)	2.072(2)
Pd1−C1	2.226(8)	2.129(2)
Pd1−C6	2.615(8)	2.766(2)
C6−O1	1.36(1)	1.236(3)
C1−C6	1.41(1)	1.495(3)
C1−C2	1.47(1)	1.483(3)
	Bond Angles	
O1L−Pd−O2L	90.6(2)	89.54(8)
O1L−Pd−C1	99.1(3)	94.38(8)
O1L−Pd−P	177.0(2)	177.83(6)
C1−Pd−P	83.0(2)	83.93(7)
C1−Pd−O2L	170.3(2)	175.10(8)
P−Pd−O2L	87.2(2)	92.09(6)

The two Pd−C bond separations, 2.226(8) and 2.129(2) Å, for **12a** and **13**, respectively, are quite different and only slightly long for Pd−C σ-bonds.[8] In the π-allyl Pd-MAP cation, **14**, the analogous Pd−C

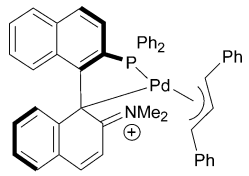

14

bond length is 2.338(11) Å, i.e., very much longer than for either **12a** or **13**.[4a] The two Pd−P bond lengths at 2.219(2) and 2.194(1) Å, for **12a** or **13**, respectively, are fairly short, as might be expected for P-donors trans to an oxygen donor.[8] The two different Pd−O separations within each complex are reasonable, although they are both significantly longer for **13** than for **12a**, in keeping with the observed difference in the Pd−C distances. The two C6−O1 distances, 1.36(1) Å for **12a** and 1.236(3) Å for **13**, clearly indicate that, in **13**, we are dealing with an organic ketone (whose expected C═O length is ca. 1.22 Å[9]). Further, for **13**, we note that the C4−C5 bond length, at 1.331(4) Å,[9] is consistent with the localized C═C bonding found in **9**. The Pd−C1−C1′ angles of 113.5(5)° and 114.6(2)° in the two structures suggest some tetrahedral character for C1. Taken together these X-ray data suggest that, for complexes **12a** and **13**, C1 represents an *alkyl-like donor*. The bonding within the hydrocarbon of **12a**,**b** is best discussed together with the ^{13}C data.

NMR Solution Results. Selected ^{13}C NMR data for the ligands and their complexes, **12** and **13**, are shown in Table 2. In solution we observed only a single species for both **12** and **13**. As there is little to distinguish **12a** from **12b**, only the former will be discussed. Figures 3 and 4 show the ^{13}C,^{1}H long-range correlations which provide the key assignments for the fully substituted carbon resonances. The proton AX spin system, from the signals for H4 and H5, is readily assigned via COSY

Table 2. δ ^{13}C (in ppm) for the Complexes and Ligands

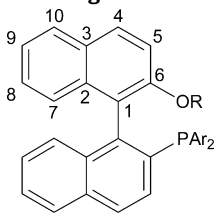

position	10a	12a	10b	12b	11	13
C1	122.1	86.7	122.2	86.9	118.3	70.5
C2	134.4	140.2	134.2	139.8	133.7	146.1
C3	129.1	129.5	128.9	129.3	128.8	128.8
C4	130.2	147.1	130.0	146.9	130.2	142.8
C5	113.0	113.3	113.5	113.4	117.7	127.6
C6	155.5	166.3	155.1	166.4	151.4	193.7
C7	125.4	125.9	*a*	126.3	125.0	126.5
C8	126.8	131.4	*a*	*a*	126.8	127.9
C9	123.7	127.4	*a*	*a*	123.4	123.9
C10	128.3	130.4	127.8	130.3	128.2	128.7

[a] Not assigned.

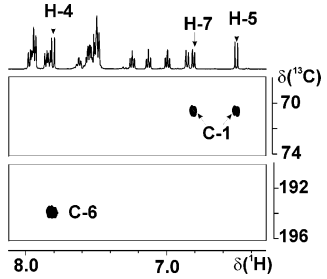

Figure 3. ^{13}C long-range correlation for **13**. The chemical shift of the ketone C═O is clearly revealed by the correlation to H4, whereas H5 and H7 correlate to the pseudo-sp^3 carbon, C1, (CD_2Cl_2).

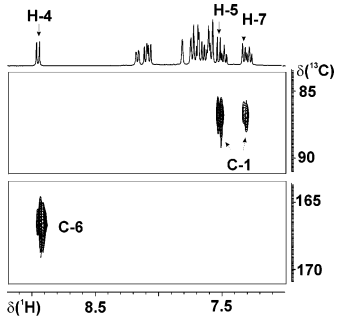

Figure 4. ^{13}C long-range correlation for **12b**. The chemical shift of the MeO−C ipso-carbon, C6, resonance is clear, at δ = 166.4, via the correlation to H4, whereas H5 and H7 correlate to the pseudo-sp^3 carbon, C1, (CD_2Cl_2).

spectroscopy. Further, the second AX pattern (in the phosphine naphthyl moiety) is readily detected via a ^{31}P,^{1}H correlation and thus is easily differentiated from H4 and H5. One can also use the ^{3}J(C6,H(MeO)) interaction to confirm the assignment of C6.

The ketone carbon in **13**, at δ = 193.7, is readily observed (see Figure 3) and found at a much higher frequency than one would expect for a phenolic sp^2 carbon. Moreover, the organic ^{13}C NMR literature[11,12]

(8) Orpen, A. G.; Brammer, L.; Allen, F. H.; Kennard, O.; Watson, D. G.; Taylor, R. *J. Chem. Soc., Dalton Trans.* **1989**, S1−S83.
(9) Allen, F. H.; Kennard, O.; Watson, D. G.; Orpen, A. G.; Brammer, L.; Taylor, R. *J. Chem. Soc., Perkin Trans. 2* **1987**, S1−S19.

(10) During the preparation of the manuscript Chan and co-workers published the preparation of a related ketone-like Pd-complex, based on a di-imine ligand: Xu, L.; Shi, Q.; Li, X.; Jia, X.; Huang, X.; Wang, R.; Zhou, Z.; Lin, Z.; Chan, A. S. C. *Chem. Commun.* **2003**, 1666−1667.

Scheme 4. Δ(δ ^{13}C) Values (in ppm) for Compounds 12a and 13, Δ(δ ^{13}C) = δ ^{13}C(coordinated ligand) − δ ^{13}C(free ligand)

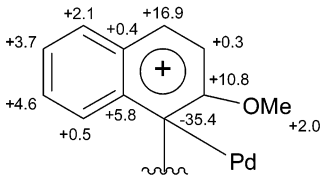

12a

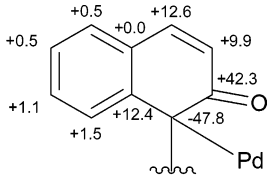

13

suggests that this is exactly the correct δ value for the carbonyl of an α,β-unsaturated ketone.

For both **12a** and **13** the ipso carbons, C1, involved in the Pd bonding, appear at low frequency, δ = 86.7, 70.5, respectively, in the aliphatic region of the spectrum, thereby supporting their formulation as pseudo sp^3 carbons. As expected, based on the relatively short Pd−C bond length in **13**, this C1 resonance appears at the lowest frequency.

Salt **12a** contains a primarily organic cation, in that, formally, the local coordination sphere about the Pd atom is neutral. The ^{13}C signal of the β-carbon of an

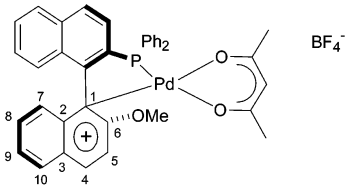

12a

α,β-unsaturated organic ketone or ester should be found at ca. 140−150 ppm,[11,12] so that the observed chemical shift value of C4, 142.8 ppm, in **13** is as expected. However, the observed chemical shift of 147.1 ppm for

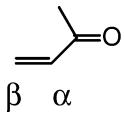

C4 in **12a** suggests that this carbon carries some of the cation positive charge (see Scheme 4 and Table 2). Scheme 4 gives the ^{13}C coordination chemical shifts for **12a** and **13**. These data reveal relatively large Δδ values for the resonances of C4 and C6 in **12a**, 16.9 and 10.8 ppm, respectively.

Continuing for **12a**, the methoxy-bearing carbon, C6 at 166.3 ppm (rather than at 155.5 as found in the ligand itself), appears at relatively high frequency, suggesting that this carbon position, along with C4 and C6, also shares in the positive charge of the cation.

We note that the ^{31}P chemical shifts for **12a** and **13**, δ = 48.5, 46.5, respectively, appear at considerably higher frequency than for *trans*-PdCl$_2$(**10**)$_2$, δ = 29.7.

Comments. It seems clear that the MOP class will find one of several possible chelating modes with which to complex Pd(II) when given the opportunity. The presence of either of the electron-donating substituents, Me$_2$N or MeO, can lead to molecular structures, in both the solid and solution states, that favor a σ-bond between C1 and the Pd atom. If the MOP oxygen atom carries an H atom, this is readily lost to afford the keto-anion. The keto-anion structure is easily recognized via its characteristic ^{13}C carbonyl chemical shift. Since the parent MOP ligand, **3** in Scheme 1, may not readily form structures such as **12** or **13**, it seems likely that individual ligands within the MOP class may well behave quite differently under catalytic conditions. With respect to how the MOP class functions as a chiral auxiliary, it remains to be seen whether more than one MOP ligand prefers to complex a transition metal, and studies in this direction are in progress.

Experimental Section

All manipulations were carried out under a nitrogen atmosphere. Pentane and ether were distilled from NaK, and CH_2Cl_2 from CaH_2. The (R)-MOP ligands were prepared by published procedures.[13] Pd(acac)$_2$ was purchased from Strem. [Pd(acac)(CH$_3$CN)$_2$](BF$_4$) was prepared by reaction of Pd(acac)$_2$ with 1 equiv of HBF$_4$ in CH$_3$CN. NMR spectra were recorded with Bruker DPX-400 and DPX-500 spectrometers at room temperature. Chemical shifts are given in ppm and coupling constants (*J*) in hertz. Elemental analyses and mass spectroscopic studies were performed at the ETHZ.

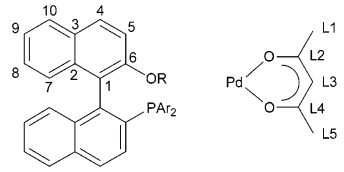

Numbering scheme for NMR assignments:

Crystallography. Air-stable, red crystals of **12a**[BF$_4$]·(CH$_3$)$_2$CO were obtained from CH_2Cl_2/ether. Dark orange crystals of **13**·CH_2Cl_2, suitable for X-ray diffraction, were obtained by crystallization from CH_2Cl_2/pentane and are air stable.

For the data collection, prismatic single crystals of both compounds were mounted on a glass fiber at a random orientation. For compound **12a** a Bruker SMART CCD diffractometer was used for a room-temperature data collection. For **13**, data were acquired at 90(2) K using a Bruker APEX CCD diffractometer. The space groups were determined from the systematic absences, while the cell constants were refined with the data reduction software SAINT[14] at the end of the data collection. The experimental conditions for the data collection, plus crystallographic and other relevant data, are listed in Tables 3 and S1.

The collected intensities were corrected for Lorentz and polarization factors[14] and empirically for absorption using the SADABS program.[15] The standard deviations on intensities were calculated in term of statistics alone, while those on F_o^2 were calculated as shown in Table 3 and Table S1.

Structural Study of 12a[BF$_4$]·(CH$_3$)$_2$CO. The structure was solved by direct and Fourier methods and refined by full matrix least squares,[16] minimizing the function $[\sum w(F_o^2 - (1/k)F_c^2)^2]$ and using anisotropic displacement parameters for

(11) Kalinowski, H. O.; Berger, S.; Braun, S. *^{13}C NMR Spektroskopie*; Georg Thieme Verlag: Stuttgart, 1984.
(12) Pretsch, E.; Seibl, J.; Simon, W. *Strukturaufklarung organischer Verbindungen*; Springer-Verlag: Berlin, 1986.
(13) Uozumi, Y.; Tanahashi, A.; Lee, S.; Hayashi, T. *J. Org. Chem.* **1993**, 1945−1948.
(14) *SAINT: SAX Area Detector Integration*; Siemens Analytical Instrumentation, 1996.
(15) Sheldrick, G. M. *SADABS*; Universität Göttingen. To be published.
(16) Sheldrick, G. M. *SHELX-97. Structure Solution and Refinement Package*; Universität Göttingen, 1997.

Table 3. Experimental Data for the X-ray Diffraction Study of Compounds 12a[BF_4]·($(CH_3)_2CO$ and 13·CH_2Cl_2

formula	$C_{41}H_{38}BF_4O_4PPd$	$C_{38}H_{32}Cl_2O_3PPd$
mol wt	818.89	744.91
data coll. *T*, K	293(2)	90(2)
diffractometer	Brucker SMART	Brucker APEX
cryst syst	orthorombic	monoclinic
space group (no.)	$P2_12_12_1$ (19)	$P2_1$ (4)
a, Å	9.082(2)	8.7586(4)
b, Å	18.718(5)	17.9736(8)
c, Å	22.526(6)	11.2010(5)
β, deg		112.061(1)
V, Å^3	3829(2)	1634.2(1)
Z	4	2
$\rho_{(calcd)}$, g cm^{-3}	1.420	1.514
μ, cm^{-1}	5.86	8.18
radiation	Mo Kα (graphite monochrom., $\lambda = 0.71073$ Å)	
θ range, deg	$2.11 < \theta < 26.27$	$2.27 < \theta < 27.54$
no. data collected	20 744	17 143
no. indep data	6843	7471
no. obsd reflns (n_o) $[\lvert F_o\rvert^2 > 2.0\sigma(\lvert F\rvert^2)]$	4632	7222
no. of params refined (n_v)	431	415
R_{int}	0.0705	0.0272
R(obsd reflns)[a]	0.0587	0.0281
R_w^2(obsd reflns)[b]	0.1071	0.0649
[c]GOF	1.038	1.046

[a] $R = \sum(\lvert F_o\rvert - (1/k)\lvert F_c\rvert)/\sum\lvert F_o\rvert$. [b] $R_w^2 = [\sum w(F_o^2 - (1/k)F_c^2)^2/\sum w\lvert F_o^2\rvert^2]$. [c] GOF $= [\sum_w(F_o^2 - (1/k)F_c^2)^2/(n_o - n_v)]^{1/2}$.

all atoms. In the difference Fourier maps a clathrated acetone molecule was located and refined using isotropic temperature factors. Both the acetone molecule and the BF_4^- anion are highly disordered, as can be seen from the large atomic displacements, and therefore their geometries are only approximate. It proved impossible to find a reasonable model for the disorder of the counterion, so that it was constrained to maintain a tetrahedral geometry. No extinction correction was deemed necessary. Upon convergence (see Table S1), the final Fourier difference map showed no significant peaks. The contribution of the hydrogen atoms, in their calculated position (C−H = 0.95 (Å), B(H) = 1.2/1.5B(C_{bonded}) (Å^2)), was included in the refinement using a riding model. Refining the Flack's parameter[17] tested the handedness of the structure.

Structural Study of 13·CH_2Cl_2. The structure was solved and refined as above. Anisotropic displacement parameters were used for all atoms. A clathrated solvent molecule (CH_2Cl_2) was found from the difference Fourier maps and included in the refinement. The solvent molecule is disordered over two positions. Both orientations were refined together with their occupancy factors (0.81 and 0.19, respectively), using anisotropic ADPs. The handedness of the structure was tested by refining the Flack's parameter.[17] All calculations were carried out by using the PC version of SHELX-97.[16] The scattering factors used, corrected for the real and imaginary parts of the anomalous dispersion, were taken from the literature.[18]

Synthesis of [(10a)Pd(acac)](BF_4), 12a. To a stirred solution of 40 mg (0.107 mmol) of [Pd(acac)($CH_3CN)_2$](BF_4) in 3 mL of acetone and 1 mL of CH_2Cl_2 was slowly added 50 mg (0.107 mmol) of **10a** in 3 mL of acetone at room temperature. Stirring was continued for 15 min, followed by removal of the solvents under reduced pressure. The crude product was recrystallized from CH_2Cl_2/ether and washed twice with ether (10 mL portions). Yield: 70.7 mg (87%). Anal. Calcd for $C_{38}H_{32}O_3BF_4PPd$ (760.87): C, 59.99; H, 4.24. Found: C, 59.72; H, 4.48. MS (MALDI): 673.1 ($M^+ - BF_4$, 100%), 574.1 ($M^+ - BF_4$ − acac, 32%). ^{1}H NMR (CD_2Cl_2, 400 MHz): 8.84 (d, $^3J_{HH}$ = 9.3, *H-4*), 7.98 (d, $^3J_{HH}$ = 7.8, *H-10*), 7.48 (*H-9*), 7.42 (*H-8*), 7.39 (d, $^3J_{HH}$ = 9.3, *H-5*), 7.23 (d, $^3J_{HH}$ = 8.2, *H-7*), 5.04 (s, *L3-H*), 3.60 (s, O-CH_3), 1.73 (s, *L1-C*H_3), 1.67 (s, *L5-C*H_3). ^{13}C NMR (CD_2Cl_2, 100 MHz): 188.7 (*L2-C*), 184.9 (*L4-C*), 99.5 (*L3-C*), 57.7 (O-*C*H_3), 28.4 (*L1-C*), 26.1 (*L5-C*). For additional ^{13}C data, see Table 2. ^{31}P NMR (CD_2Cl_2, 161 MHz): 48.5 (s).

Synthesis of [Pd(acac)(10b)](BF_4), 12b. To a stirred solution of 17.3 mg (0.046 mmol) of [Pd(acac)($CH_3CN)_2$](BF_4) in 1.5 mL of acetone was slowly added a solution of 32 mg of **10b** in 3 mL of CH_2Cl_2. The resulting solution was stirred for 10 min at room temperature, followed by removal of the solvents under reduced pressure. The red solid obtained was washed twice with pentane. Yield: 44 mg (97%). Anal. Calcd for $C_{54}H_{64}O_3BF_4PPd·H_2O$ (1003.32): C, 64.64; H, 6.63. Found: C, 64.64; H, 6.59. MS (HiResMALDI): found 897.3651 ($M^+ - BF_4$, 100%), calcd 897.3641. ^{1}H NMR (CD_2Cl_2, 500 MHz): 8.96 (d, $^3J_{HH}$ = 9.4, *H-4*), 8.10 (d, $^3J_{HH}$ = 8.0, *H-10*), 7.51 (d, $^3J_{HH}$ = 9.4, *H-5*), 7.30 (d, $^3J_{HH}$ = 8.3, *H-7*), 5.13 (s, *L3-H*), 3.78 (s, O-CH_3), 1.86 (s, *L1-C*H_3), 1.75 (s, *L5-C*H_3), 1.33 (s, 18 H, C(CH_3)$_3$), 1.31 (s, 18 H, C(CH_3)$_3$). ^{13}C NMR (CD_2Cl_2, 125 MHz): 187.7 (*L2-C*), 184.4 (*L4-C*), 99.4 (*L3-C*), 58.5 (O-*C*H_3), 34.9 (*C*(CH_3)$_3$), 30.9 (C(*C*H_3)$_3$), 28.5 (*L1-C*), 26.2 (*L5-C*). For additional ^{13}C data, see Table 2. ^{31}P NMR (CD_2Cl_2, 202 MHz): 51.4 (s).

Synthesis of [Pd(acac)(11-H)], 13. To a stirred solution of 26.8 mg (0.088 mmol) of Pd(acac)$_2$ in 1 mL of CH_2Cl_2 was slowly added a solution of 40 mg (0.088 mmol) of **7** in 3 mL of CH_2Cl_2. The solution was stirred for 18 h at room temperature, at which point an in situ ^{31}P NMR showed one major product (ca. 95%). The solvent was evaporated under reduced pressure and the crude product recrystallized from CH_2Cl_2/pentane. The product was washed twice with pentane. Yield: 32 mg (55%). Anal. Calcd for $C_{37}H_{29}O_3PPd$ (659.03): C, 67.43; H, 4.44. Found: C, 67.27; H, 4.60. MS (MALDI): 559 (M^+ − acac, 35%), 453 (HO-MOP, 100%). ^{1}H NMR (CD_2Cl_2, 500 MHz): 7.81 (d, $^3J_{HH}$ = 9.7, *H-4*), 7.49 (*H-10*), 7.13 (t, $^3J_{HH}$ = ca. 7.3, *H-9*), 6.99 (t, $^3J_{HH}$ = ca. 7.3, *H-8*), 6.81 (d, $^3J_{HH}$ = 7.7, *H-7*), 6.51 (d, $^3J_{HH}$ = 9.7, *H-5*), 5.16 (s, *L3-H*), 1.83 (s, L1-CH_3), 1.79 (s, L5-CH_3). ^{13}C NMR (CD_2Cl_2, 125 MHz): 187.1 (*L2-C*), 186.0 (*L4-C*), 98.9 (*L3-C*), 28.2 (*L1-C*), 27.4 (*L5-C*). For additional ^{13}C data, see Table 2. ^{31}P NMR (CD_2Cl_2, 202 MHz): 46.5 (s).

Acknowledgment. P.S.P. thanks the Swiss National Science Foundation and the ETH Zurich for financial support. A.A. thanks MIUR for a research grant (PRIN 2002). We also thank Johnson Matthey, U.K., for the loan of precious metal salts.

Supporting Information Available: Text giving experimental details and a full listing of crystallographic data, including tables of positional and isotropic equivalent displacement parameters, calculated positions of the hydrogen atoms, anisotropic displacement parameters, bond distances, bond angles, and torsion angles. ORTEP figures showing the full numbering schemes. This material is available free of charge via the Internet at http://pubs.acs.org.

OM030555D

(17) Flack, H. D. *Acta Crystallogr.* **1983**, *A 39*, 876.
(18) *International Tables for X-ray Crystallography*; Wilson, A. J. C., Ed.; Kluwer Academic Publisher: Dordrecht, The Netherlands, 1992; Vol. C.